JOURNAL OF APPLIED ELECTROCHEMISTRY 5 (1975) 305–312

Comparative investigations of packed and fluidized bed electrodes with non-conducting and conducting particles

G. KREYSA, S. PIONTECK, E. HEITZ

Dechema-Institut, D-6000 Frankfurt/Main, Theodor-Heuss-Allee 25, Federal Republic of Germany

Received 29 September 1974

Current density-potential curves and the dependency of current density on flow velocity were measured for reaction systems which are controlled by diffusion in packed and fluidized bed electrodes with conducting and non-conducting particles. Analogous measurements were carried out with plane electrodes, and the corresponding dependencies of the current density factor i_b/i_{pl} were determined. For bed electrodes with conducting particles, the current density factor can be approximately described as the product of a surface scale-up factor and a diffusion-controlled factor of the order of 5. Parallel to the current flow direction, the effectiveness of a bed electrode with conductive particles covers only a layer thickness of less than 1 cm. Maximum current densities are found with both conducting and non-conducting particles at flow velocities above the fluidization point.

Nomenclature

A – surface area of all particles per unit volume (cm^{-1})
d – particle diameter (cm)
f_c – current density factor
f_c^d – diffusion-determined current density factor
f_c^s – surface scale-up factor
F_s – bed cross-section (cm^2)
h – bed height (mm)
h_0 – static bed height (mm)
h_{eff} – effective bed height (mm)
I – current (A)
i_b – current density of bed electrode ($\mathrm{A\,cm}^{-2}$)
i_{pl} – current density of plane electrode ($\mathrm{A\,cm}^{-2}$)
V – bed voidage
v – flow velocity ($\mathrm{cm\,s}^{-1}$)
v_m – flow velocity at the maximum of current density ($\mathrm{cm\,s}^{-1}$)
η – overvoltage (mV)

1. Introduction

Three-dimensional electrode systems such packed and fluidized bed electrodes are winning increasing technical importance as they allow the application of considerably higher current densities than two-dimensional electrodes, and the ratio between electrochemical conversion and cell volume can become very great. If one considers, for example, a fluidized bed electrode of conducting particles in which a diffusion-controlled electrochemical reaction takes place, one finds that the increase in current density has two causes. Firstly, the effective electrode surface area is considerably larger than that of a two-dimensional electrode, and secondly, particle collisions and turbulences in the bed cause continuous disturbances of the diffusion layer, thus also contributing to an increase in current density. The conditions are far simpler in a fluidized bed of non-conducting particles between the electrodes. In this case, the increase in current density is exclusively due to the improvement of diffusion conditions. The first studies with electrically-conducting catalyst suspensions as electrode systems were carried out by Gerischer [1, 2]. Although there are a number of papers, mainly by Fleischmann and Goodridge, which concern themselves with fluidized beds of conducting particles [3–7], systems with non-conducting particles have only been investigated by a few workers, for example, by Le Goff [8]. There is in particular a lack of comparative investigations under as nearly as possible analogous conditions.

An important factor in assessing the efficiency of a bed electrode is the ratio of the current

Printed in Great Britain.

densities measured under identical conditions at the bed electrode and the plane electrode.

$$f_c = i_b/i_{pl}. \qquad (1)$$

In the case of a bed electrode of conducting particles, current density is to be understood as the cell current relative to 1 cm^2 bed cross-section without the feeder component.

$$i_b = \frac{I - I_{feeder}}{F_s}. \qquad (2)$$

The feeder current is measured without particles. This includes the assumption that the feeder current is identical in the presence and the absence of the conducting particles. An experimental fact giving support to this point will be discussed in Section 3.2. The factor f_c defined by Equation 1 is described as the current density factor in the following account. Although the literature already contains theoretical approaches for calculating f_c under special conditions, e.g. Fleischmann [9, 10], there is a lack of systematic investigations on the influence of various parameters on this ratio. This paper therefore compares the parameters measured at the bed electrode with the analogous results for a plane electrode, and discusses the influence of various parameters on the current density factor. Diffusion-controlled cathodic reductions are used as the reaction systems. The reaction

$$Fe(CN)_6^{3-} + e^- \longrightarrow Fe(CN)_6^{4-} \qquad (3)$$

is used as an example in determining the current density increase resulting from improved diffusion conditions in a bed of non-conducting particles. A bed of compact silver spheres in which the reaction

$$Ag^+ + e^- \longrightarrow Ag \qquad (4)$$

took place is used to investigate the properties of bed electrodes of conducting particles. Not only the fluidized bed was investigated; the measurements were also extended to cover the packed bed. The precise experimental investigation of the influence of various conditions on current density which can be achieved in a bed electrode is one of the main prerequisites for assessing the possibilities and limitations of technical utilization of such electrode systems.

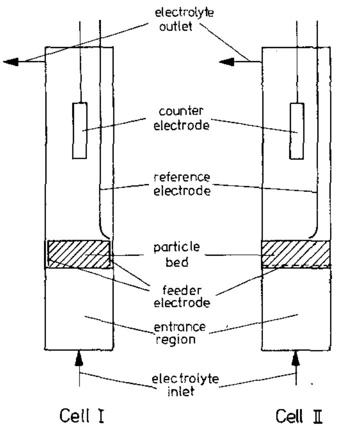

Fig. 1. Construction of the cells. Cell I: bed with glass spheres; Cell II: bed with solid silver spheres.

2. Experimental

2.1. *Apparatus and cells*

The main component of the electrolyte flow circuit is a rectangular flow channel of 7·69 cm^2 cross-section in which the electrode arrangement is mounted. Cell I in Fig. 1 was employed for measurements with non-conducting particles. Its working electrodes consist of 20 mm-high platinum plates mounted in the sides of the flow channel. The static bed height is identical with the height of the working electrodes. Glass spheres with diameters of 0·95, 0·70, 0·45, and 0·27 mm were used as particles. The reference electrode consisted of platinum wire in a Luggin capillary mounted near the working electrode. Cell II was used for the measurements with conducting particles. The bed consisted of silver spheres of 1 mm diameter (provided by Messrs Degussa of Hanau/GFR) on a platinum mesh which acted as the feeder electrode. The reference electrode was a silver wire in a Luggin capillary which was placed near the top of the bed. The counter-electrode in both cells was a platinum mesh cylinder above the bed. To achieve uniform fluidization of the bed, the electrolyte first flows through a 140 mm-long entrance region which was filled with glass spheres of 0·7 mm diameter. With this arrangement throughout the experiments, no entrance region effect in respect to the total bed behaviour could be observed (for further details see Fig. 8 in Section 3.2). The above-mentioned electrode arrangement in Cell II could also be replaced by two electrodes mounted parallel to the flow direction to obtain measurements at the plane electrode under otherwise-identical conditions. The working electrode here consisted of a silver plate of 4 cm^2 area; the counter-electrode was a platinum plate.

The measurements were carried out with potentiostatic control of the potential between reference electrode and feeder (potentiostat 70 HC 3, Messrs G. Bank Elektronik, Göttingen, GFR). Preliminary experiments indicated the advisability of polarizing the electrode for 2 min before each measuring point with a saw-tooth waveform (scan rate: 1 V s^{-1}) of ± 100 mV (relative to the equilibrium potential of the electrode in the electrolyte used) to maintain readily-reproducible conditions. The temperature during all measurements was 25°C.

2.2. *Electrolytes*

The electrolyte used in the investigation of Reaction 3 in Cell I was: $2 \cdot 10^{-4}$ M $K_3Fe(CN)_6$ + $2 \cdot 10^{-3}$ M $K_4FeCN)_6$ + $2 \cdot 10^{-2}$ M NaOH. In Cell II, Reaction 4 was investigated with a solution of 10^{-3} M $AgNO_3$ + 0·5 M KNO_3 as electrolyte.

3. Results and discussion

3.1. *Non-conducting particles*

In order to determine whether the increase in current density in a bed electrode of conducting particles can be quantitatively attributed to the two effects of surface enlargement and the improvement of diffusion conditions, it is necessary to first separately investigate the influence of the fluidized bed on diffusion. The arrangement of Cell I with a bed of non-conducting particles is used for this purpose. The test reaction used was the cathodic reduction of ferricyanide, which is known to be purely diffusion-controlled [11]. Fig. 2 shows the cathodic current density-potential curve with and without particles between the electrodes, at a flow velocity which is above that of incipient fluidization. The presence of the fluidized bed of 0·95 mm-diameter glass spheres causes a considerable increase in current density and displacement of the diffusion current range to higher overvoltages. In a bed of non-conducting particles, the current density increase is solely caused by the improvement of diffusion conditions; the current density

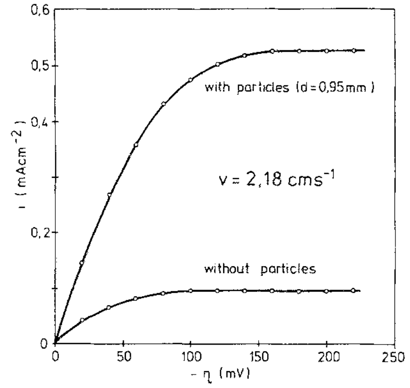

Fig. 2. Current density-potential curve of the reduction of ferricyanide with and without fluidized bed.

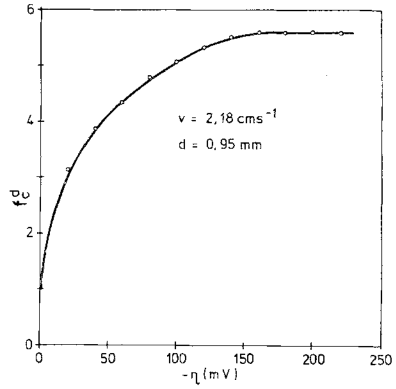

Fig. 3. Potential dependency of the current density factor f_c^d.

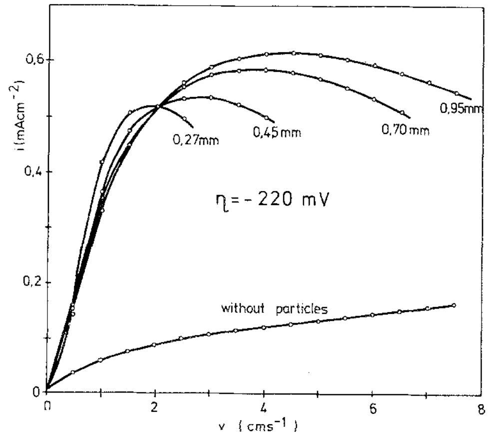

Fig. 4. Dependency of diffusion current on flow velocity for different values of particle diameter and without particles.

factor defined by Equation 1 is to be characterized with the additional index d. The potential dependency of this current density factor f_c^d is shown in Fig. 3. In the diffusion current range, f_c^d achieves a value of 5·25. This agrees well with values quoted by other authors. For the same reaction system, Le Goff *et al.* [12] quote a value of 4·3 with a flow velocity of 1·2 cm s^{-1}. In nickel deposition, the f_c^d value was 5 [8], and in copper deposition, a factor of 5–6 [13] was found. These data indicate that the factor f_c^d is independent of special properties of the reaction system in the diffusion current range.

Fig. 4 shows the dependency of the diffusion current on flow velocity for various particle diameters and a one-phase electrolyte without particles. In the case of particle-free flow, one notes the well-known proportionality to $v^{1/2}$ for a flat plate flow electrode under laminar conditions. In the presence of the particle bed, however, the current density sharply rises to a maximum which is displaced towards higher flow velocities with increasing particle diameter. The observed increase in current density is caused by the fact that the particles continually penetrate and disturb the diffusion layer. Le Goff *et al.* [12] have shown experimentally that the mean kinetic energy of all particles per unit volume rises to a maximum in a similar manner to the mass transfer coefficient under the same conditions. The existence of the maximum is thus explainable in terms of the competing effects of increased kinetic energy with increasing flow velocity and the decreasing number of particles per unit volume as the bed expansion is increased. A more detailed interpretation of this maximum and a discussion of Le Goff's hypothesis will be presented in a future paper. The abscissae of the maxima in Fig. 4 are plotted against the particle diameter on logarithmic coordinates in Fig. 5. This dependency obeys the equation

$$v_m = 23{\cdot}3d^{0{\cdot}7}. \qquad (5)$$

The influence of particle density on v_m in this equation has not been investigated and will be discussed theoretically in a future paper.

The current density factor f_c^d is shown in Fig. 6 as a function of flow velocity. One sees that the maximum of the current density factor lies at lower flow velocities than the maximum of the current density. Whilst the maximum-achievable current density increases with increasing particle diameter, the maximum current density factor is higher, the smaller the particle diameter. This is due to the shape of curves in Fig. 4.

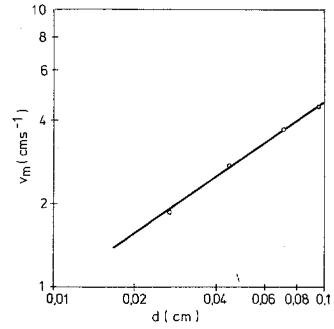

Fig. 5. Dependency of flow velocity at the current density maximum on particle diameter.

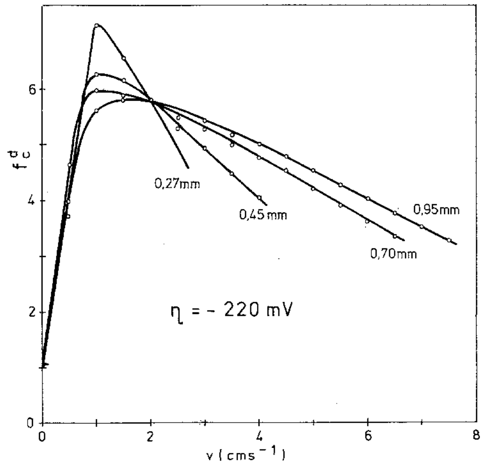

Fig. 6. Current density factor f_c^d as a function of flow velocity.

3.2. *Conducting particles*

Packed bed and fluidized bed electrodes with conducting particles offer not only better diffusion conditions than plane electrodes but also the advantage of a considerably larger electrode surface area. In the investigation of a bed electrode with conducting particles, the test reaction used was the deposition of silver from 10^{-3} M $AgNO_3$ solution in a bed of compact silver spheres of 1 mm diameter. It is known [14] that this reaction is, apart from a small crystallization overvoltage, mainly diffusion-controlled, and that practically no charge transfer control occurs as a result of a high exchange

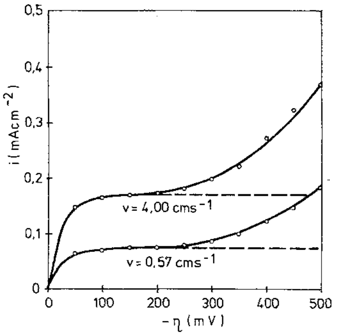

Fig. 7. Cathodic current-potential curve of the silver deposition at a plane electrode.

current density. The cathodic current density-potential curves for silver deposition at the plane electrode shown in Fig. 7 confirm this kinetic model, as one can observe the theoretical flow dependency of the limiting current. The new rise in current density in the diffusion current range is due to a reduction of the dissolved oxygen.

In Cell II (Fig. 1), current flow is parallel to the flow direction of the electrolyte. Because a potential gradient forms in the bed, no linear scale-up between bed height and current density can be expected. Only the scale-up at right-angles to the direction of current flow [3] has been experimentally investigated up till now; a linear relationship between bed length and current density was found. Only theoretical estimates are at present available for the scale-up parallel to the direction of current flow; a calculation of Fleischmann [9] indicates that increases in current density can only be expected up to a bed height of about 1 cm for a diffusion-controlled reaction. In order to determine an optimal bed height for further experiments, we therefore first investigated the influence of bed height on current density under various conditions. Fig. 8 shows current density plotted against the static bed height for various flow velocities and overvoltages. Current density here is to be understood as the expression defined by Equation 2. Under the conditions of the measurements in Fig. 8, the feeder current measured without particles had values up to 30% of the total bed current. The origin of the current density versus bed height curves is zero and the initial linear rise is also a strong argument for the fact that in the given cell construction no entrance region effect is present. An initial linear rise in Fig. 8 is followed in all cases by a maximum current density achieved at a certain bed height which in the following is described as the effective bed height (h_{eff}). Increasing bed height beyond h_{eff} is therefore not practical. The effective bed heights shown in Fig. 8 are of the same order of those estimated by Fleischmann and Oldfield [9]. A similarity law suitable for the more exact determination of effective bed height has recently been reported [15]. Fig. 8 also shows that the maximum-achievable current densities in fluidized beds are greater than those achievable in packed beds.

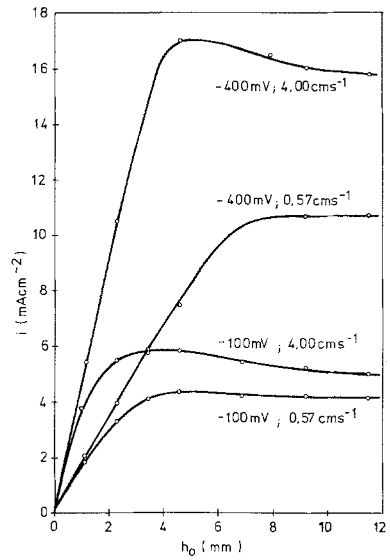

Fig. 8. Dependency of current density on static bed height at various overvoltages and flow velocities $v = 0{\cdot}57\ \mathrm{cm\,s^{-1}}$: packed bed; $v = 4{\cdot}00\ \mathrm{cm\,s^{-1}}$: fluidization point.

Fig. 9 shows the current density factor as defined by Equation 1 as a function of static bed height. One notes that greater current density factors can be achieved at constant overvoltage in the packed bed than in the fluidized bed. This indicates that an increase of flow velocity in the bed electrode causes a lesser increase in current density than at the plane electrode, which in turn allows one to conclude that the potential gradient in the bed becomes steeper with increasing flow velocity. In considering the current density factor of a bed electrode of conducting particles, one must note that the actual effective electrode surface area is considerably greater than allowed for in the definition of i_b by Equation 2. The current density factor contains a geometric scale-up factor of electrode surface area.

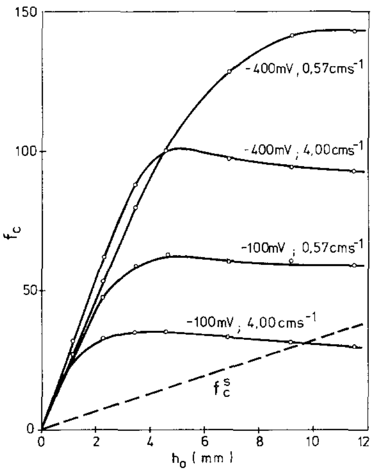

Fig. 9. Current density factor as function of static bed height (broken straight line: surface scale-up factor).

This is designated f_c^s, and represents the geometric surface of all particles within 1 cm^2 of bed cross-section. The calculation of the surface area of all spheres per unit volume gives:

$$A = \frac{6(1-V)}{d}, \qquad (6)$$

where V is the bed voidage and d the particle diameter. For a static bed height of 1 mm it follows that:

$$f_c^s(1\,\mathrm{mm}) = \frac{3(1-V)}{5d}. \qquad (7)$$

With the experimental values for V (0·46) and d (0·1 cm), one arrives at the relationship

$$f_c^s = 3{\cdot}24h \qquad (8)$$

for the bed height-dependent surface scale-up factor. This function is plotted as a broken straight line in Fig. 9.

Table 1. Quotients f_c/f_c^s at $h = h_{\mathrm{eff}}$

v(cm s^{-1})	η(mV)	f_c/f_c^s	f_c^{d*}
0·57	− 100	4·21	4·35
0·57	− 400	6·21	4·82
4·00	− 100	4·48	4·52
4·00	− 400	6·75	5·00

* Utilizing the values determined in Figs. 3 and 6.

Table 1 gives the quotients f_c/f_c^s which were derived from the values at the effective bed height for various conditions. One notes that these quotients agree quite well with the f_c^d values shown in Figs. 3 and 6. The current density factor of a bed electrode of conducting particles can therefore be estimated in the range below effective bed height by means of the simple relationship

$$f_c \approx f_c^s f_c^d \qquad (h \leqslant h_{\mathrm{eff}}). \qquad (9)$$

To avoid larger parts of the bed becoming inactive, the following measurements were carried out with a bed height of 4·6 mm. Fig. 10 shows the cathodic current density-potential curve in the packed bed area and at the fluidization point. Whilst a diffusion current is still achieved in the packed bed, it is no longer detectable within the investigated potential range in the fluidized bed. Fig. 11 shows the potential dependency of the current density factor.

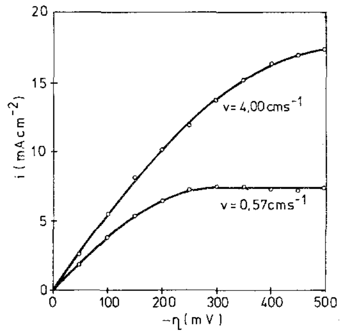

Fig. 10. Cathodic current density-potential curve of the silver deposition at the packed and fluidized bed electrode (h_0 = 4·6 mm).

Here, once again, one finds that the current density factor, unlike current density itself, is greater in the packed bed than in the fluidized bed throughout practically the entire potential range. Equation 9 indicates that the proportionality between f_c and f_c^d is to be expected for constant f_c^s. In fact, one finds that f_c in Fig. 11 increases with rising potential, as does f_c^d in Fig. 3. The flow dependency of current density at an overvoltage of − 200 mV is shown in Fig. 12 for the plane electrode and the bed electrode. Current density in the bed reaches a maximum above the fluidization point (4 cm s^{-1}). This maximum is not – as in the case of non-conducting particles – solely due to the occurrence of a maximum of kinetic energy of all particles per

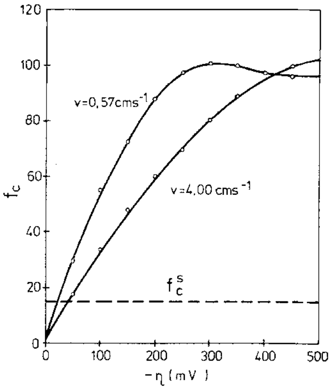

Fig. 11. Dependency of current density factor on potential for the packed and fluidized bed electrode (h_0 = 4·6 mm; broken straight line: surface scale-up factor).

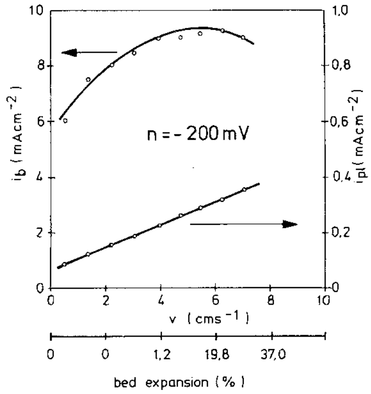

Fig. 12. Dependency of current density on flow velocity at plane electrode and bed electrode (h_0 = 4·6 mm; fluidization point = 4·00 cm s^{-1}).

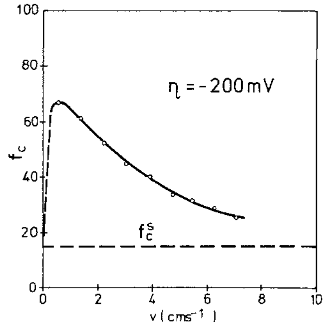

Fig. 13. Dependency of current density factor on flow velocity (h_0 = 4·6 mm; v = 4·00 cm/s; broken straight line: surface scale-up factor).

unit volume, but has a further cause. As the specific conductivity of the electrolyte is considerably lower than that of the metal phase, the effective resistance and thus the ohmic potential drop increases as the bed expands. This causes a reduction in the mean potential of the particles, which also contributes to a reduction of current density above the fluidization point. As in the other case, the current density increases with increasing flow velocity as a result of a reduction of the diffusion layer thickness; the observed maximum results from the superimposition of these tendencies. The dependency of the current density factor on flow velocity shown in Fig. 13 shows a clear analogy to the flow dependency of f_c^d in Fig. 6, as f_c^s is constant. Here once again, one finds that the current density factor reduces continuously between packed bed and fluidized bed, whilst the current density in this range increases.

4. Conclusions

Because of the high current density factor which reaches values of the order of 100, bed electrodes with conducting particles should be particularly interesting for diffusion-controlled electrochemical processes which occur particularly at low concentrations of the reacting species. The equation

$$i_b = f_c^s \cdot f_c^d \cdot i_{pl} \qquad (10)$$

allows an estimation of the current density to be expected in the bed electrode when i_{pl} is known. A value of 5 can be assumed for f_c^d within the diffusion current density range, whilst f_c^s can be simply calculated from particle diameter and bed voidage. Constructional limitations must however be observed in dimensioning the bed parallel to the direction of the current flow, these being given by the effective bed height of approximately 0·5–3 cm. As the current density factor – unlike current density itself – is greater in the packed bed than in the fluidized bed, the question of the most economic operating conditions of the bed electrode cannot be immediately answered in favour of the fluidized bed electrode if one allows for the fact that the maintenance of the bed gives rise to additional energy costs.

Acknowledgements

We wish to express our thanks to the Deutsche

Forschungsgemeinschaft for the financial support given to our work.

References

[1] H. Gerischer, *Ber. Bunsenges. physik. Chem.* **67** (1963) 164.

[2] J. Held and H. Gerischer, *ibid* 921.

[3] J. R. Backhurst, J. M. Coulson, F. Goodridge, R. E. Plimley and M. Fleischmann, *J. Electrochem. Soc.* **116** (1969) 1600.

[4] M. Fleischmann, J. W. Oldfield and L. Tennakoon, *J. Appl. Electrochem.* **1** (1971) 103.

[5] L. J. J. Janssen, *Electrochim. Acta* **16** (1971) 151.

[6] J. N. Hiddleston and A. F. Douglas, *ibid* **15** (1970) 431.

[7] F. Goodridge, D. I. Holden, H. D. Murray and R. E. Plimley, *Trans. Instn. Chem. Engrs.* **49** (1971) 128; F. Goodridge and B. M. Ismail; *Instn. Chem. Engrs. Symp. Ser. No. 37* **1** (1973) 129.

[8] F. Vergnes, C. Verrel and P. Le Goff, *Corrosion (Paris)* **17** (1969) 131.

[9] M. Fleischmann and J. W. Oldfield, *J. Electroanal. Chem.* **29** (1971) 211, 231; D. C. Carbin and D. R. Gabe, *Electrochim. Acta* **19** (1974) 645.

[10] M. Fleischmann, J. W. Oldfield and D. F. Porter, *ibid* 241.

[11] O. Esin, S. Derendjajew and N. Ladygin, *J. Appl. Chem. (USSR)* **13** (1940) 971.

[12] P. Le Goff, F. Vergnes, F. Coeuret and J. Bordet, *Ind. Engng. Chem.* **61** (1969) (10)8; F. Coeuret and P. Le Goff, *Chem. Eng.* (1967) CE 75.

[13] R. Thangappan, B. Krishnamurthy and S. Sampath, *Metal Finish* **69** (1971) (12) 43, 49.

[14] H. Gerischer and R. P. Tischer, *Z. Elektrochem.* **61** (1957) 1159.

[15] G. Kreysa and E. Heitz, 'Kinetic Investigation into Silver Deposition at a Fluidized and Packed Particle Electrode', Joint Meeting on Cell Design in Electrowinning and Electrorefining, Southampton, July 1974. *Chem. and Ind.* (1975) 332.